

# 2nd FEASIBILITY STUDY of a MUON STORAGE RING $\nu$ FACTORY \*

S. Ozaki, R. B. Palmer, BNL, Upton, NY 11973-5000 U.S.A

M. S. Zisman, LBNL, Berkeley, CA 94720 U.S.A

for the Neutrino Factory and Muon Collider Collaboration[1]

## Abstract

The design and simulated performance of a second feasibility study are presented. The efficiency of producing muons is  $\approx 0.17 \mu/\text{p}$  with 24 GeV protons. This study was sponsored by the BNL Director, with BNL site specific driver and layout. It was a follow on to the First Study[2] sponsored by the Fermilab Director, with Fermilab site specific driver and layout, and was the main US collaboration conceptual effort during the past year. Other studies, and technical work by the collaboration is reported in other papers.

## 1 INTRODUCTION

A second feasibility study was commissioned by the Brookhaven National Lab Director, John Marburger and was presented to him on May 4 2001. It was a follow on to the study commissioned by the Fermi Lab Director FNAL specific (Study 1) that was presented in April 2000 [2] In each study there are site specific

\* work supported by US Department of energy, Division of High Energy Physics, contracts No. DE-AC02-98CH10886 and DE-AC03-76SF00098.

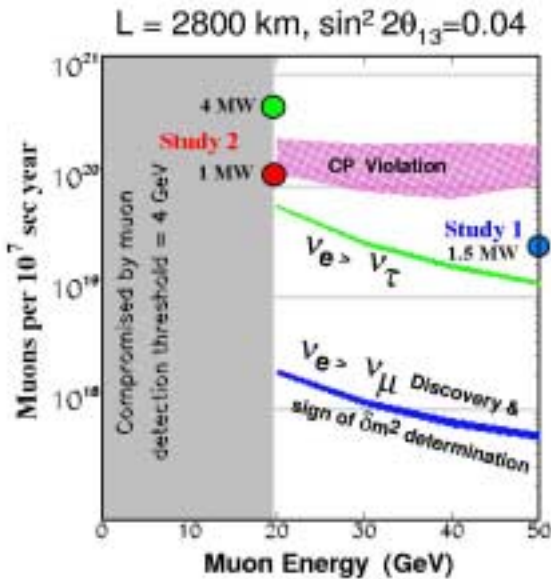


Figure 1: Muon decays in a straight section per  $10^7$  sec vs. muon energy, with fluxes required for different physics searches assuming a 50 kT detector; together with the simulated performance of the two studies.

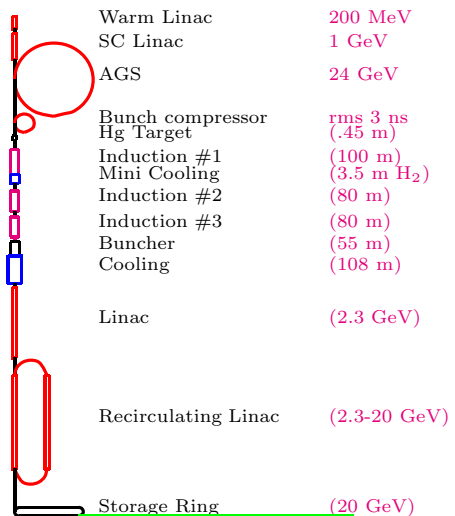


Figure 2: Schematic of System.

parts, the driver and storage ring angle, in particular, that are for the Fermilab location and BNL sites respectively. Otherwise the studies are generic with the primary difference that the second study is aimed at a lower muon energy (to save cost), but higher intensity (for physics reach: see fig.1, adapted from a physics overview [3]). Both studies were carried out under the auspices of the Muon Collider Collaboration [1] which has over 140 members from many institutions in the U.S. and abroad. The components of the system are shown schematically in fig.2.

## 2 COMPONENTS

### 2.1 Proton driver

The proton driver is an upgrade (fig.3) of the Brookhaven Alternating Gradient Synchrotron (AGS) and uses many of the existing components and facilities. The current booster is replaced by a 1.3 GeV Superconducting proton linac. The repetition rate is increased from 0.5 Hz to 2.5 Hz. The total proton charge is increased by 30% to  $10^{14}$  ppp. The 6 bunches would be extracted separately, spaced by 20 msec., so that the target, induction linacs and rf systems that follow, need only be designed to deal with single bunches at an average repetition rate of 15 Hz. The average power would be 1 MW. An upgrade to  $2 \cdot 10^{14}$  ppp and 5 Hz

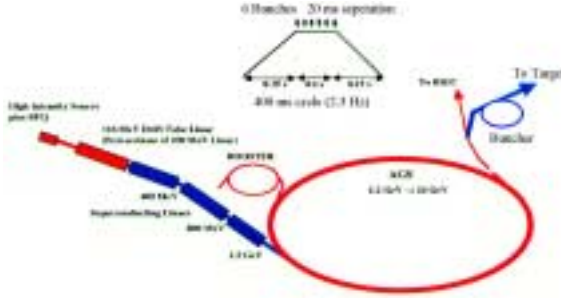


Figure 3: Proton Driver Schematic

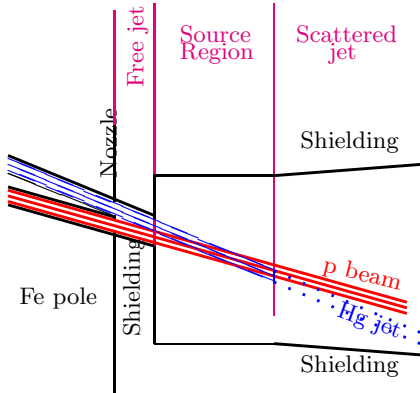


Figure 4: Mercury jet target geometry.

could give an average beam power of 4 MW.

## 2.2 Target & Capture

A high Z (mercury) target is chosen to give a high yield of pions per incident proton power ( $\approx 1.9 \times$  that for carbon). Solid metal targets could be used, but would need to be mechanically moved to avoid excessive temperatures and would have limited lifetime.

The jet is continuous, is 1 cm diameter, and enters the target enclosure at 100 mrad from the axis. The proton beam intersects the jet at an angle of 33 mrad (67 mrad from the axis). The geometry is shown in fig.4. It is assumed that the thermal shock from the interacting proton bunch fully disperses the mercury. In this case the jet must have a velocity of 30 m/sec to be replaced before the next bunch. Perturbations to the jet by the capture magnetic field are controlled by placing the jet nozzle inside the field, so that the jet only sees 1 T field changes before it has passed beyond the production region.

Pions emerging from the target are captured and focused down the decay channel by a solenoidal field that is 20 T at the target center, and tapers down, over 18 m, to a periodic (50 cm) superconducting solenoid channel (ave. field  $\approx 1.25$  T) that continues through the phase rotation to the start of bunching.

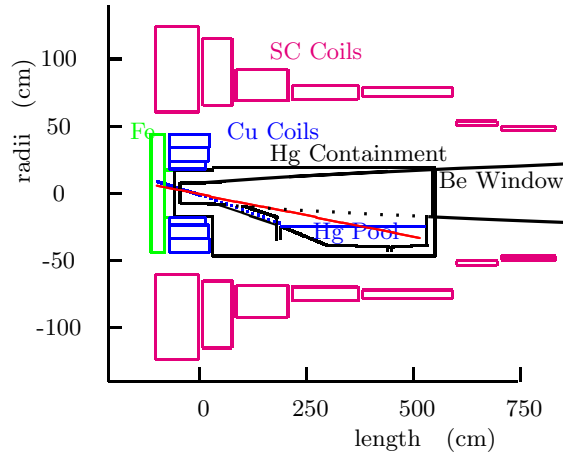


Figure 5: Mercury enclosure, mercury pool beam dump, and solenoid capture magnets.

Fig.5 shows a section of the 20 T hybrid magnet, the front end of the taper, the mercury containment, and mercury pool proton beam dump. The 20 T solenoid, with hollow copper insert and superconducting outer-sert, is not different in character to the higher field (up to 45 T), but smaller bore, magnets at several existing labs. However, the copper insert in this design is made with hollow copper conductor and ceramic insulation to withstand radiation. MARS[4] simulations of radiation levels show that, with the shielding provided, both copper and superconducting magnets should have a lifetime greater than 20 years at 1 MW.

## 2.3 Phase Rotation

Pions, and the muons into which they decay, are generated in the target over a very wide range of energies, but in a short time pulse (rms 3 ns). This large energy phase is "rotated" into a longer time phase using drifts and induction linacs. The muons first drift to spread out their time, the induction linacs then decelerate the early ones and accelerate those later. 3 induction linacs (with lengths 100, 80, and 80 m) are used in a system that reduces distortion[5] in the phase rotated bunch, and allows all induction units to operate with unipolar pulses. The 1.25 T beam transport solenoids are placed inside the induction cores to avoid saturating the ferrite. The induction units are similar to those being built for DARHT[7]. Fig.6a shows a schematic of the three units, and fig.6b gives the pulse shapes.

Between the first and second induction linacs, two hydrogen absorbers (each 1.7 m long and 30 cm radius), with a field reversal between them, are introduced to reduce the transverse emittance (mini-cooling).

Fig.7a shows distribution of pions before phase rota-

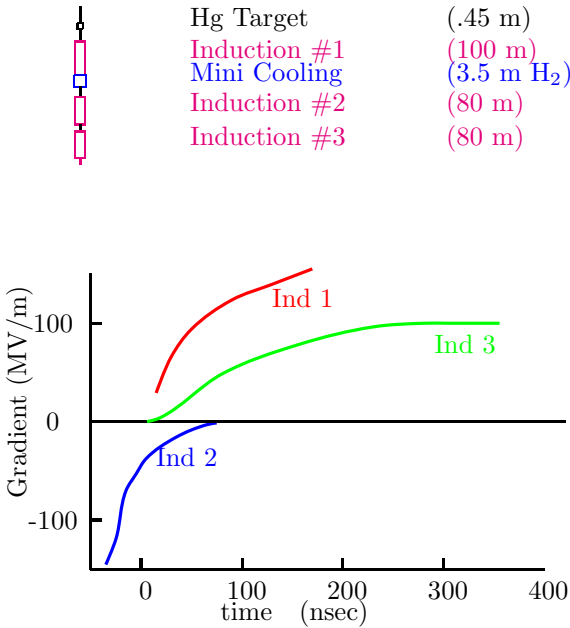


Figure 6: a) TOP: Schematic of Phase Rotation; b) BOTTOM: Pulse shapes of the 3 induction linacs.

tion. Fig.7b shows distribution of pions after the phase rotation. It is seen that after rotation, 0.5 muons per initial proton are within a band with an rms momentum spread of 4.4%, compared with the initial spread of 55%.

## 2.4 Buncher

The long bunch (400 nsec) after the phase rotation is bunched at 201 MHz prior to cooling and acceleration at that frequency. The bunching is done in a lattice identical to that at the start of cooling (see below), and is preceded by a matching section from the 1.25 T solenoids into this lattice. The bunching has three stages, each consisting of RF (with increasing acceleration) followed by a drifts with decreasing length. In the first two RF sections, second harmonic RF is used together with the 201 MHz to improve the capture efficiency.

## 2.5 Cooling

Transverse emittance cooling is achieved by lowering the beam energy in hydrogen absorbers, interspersed with RF acceleration to keep the average energy constant. Transverse and longitudinal momenta are lowered in the absorbers, but only the longitudinal mo-

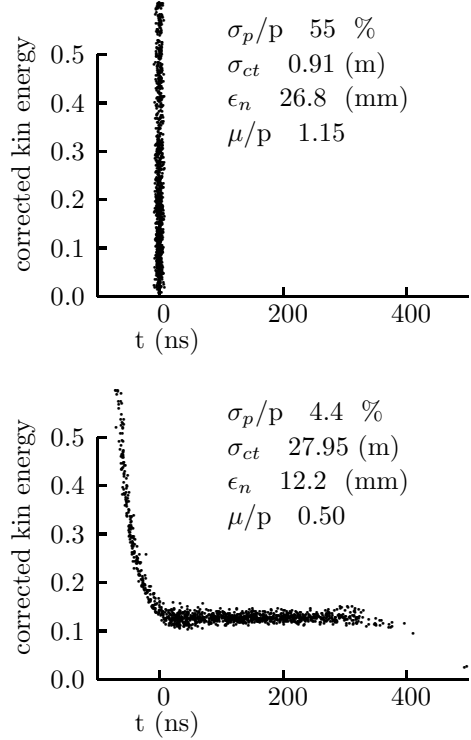


Figure 7: Phase Rotation: The kinetic energy vs. time, before (a: TOP) and after (b: BOTTOM) the phase rotation

mentum is increased by the RF. Emittance increase from Coulomb scattering is minimized by maintaining the focus strength so that the angular spread of the beam is constant and large. To achieve this, the focus strength  $\beta$  must be small and proportional to the emittance; i.e. falling as the emittance is cooled. A simple strong solenoid, with increasing field could achieve this, but such a field must be reversed periodically to avoid a growth of angular momentum. Instead, a tapered alternating field solenoid (SFOFO)[6] lattice is employed. The field shape is chosen to maximize the momentum acceptance ( $\pm 22\%$ ) and provide  $\beta$ 's (varying from 0.5 m to 0.2 m).

Fig.8 shows the initial axial field vs. length, and fig.9 shows the  $\beta$  functions vs. momentum at the start and end. Fig.11 shows the simulated emittance as it falls as a function of length. Fig.10 shows an engineering section of a cell at the end of the channel.

## 2.6 Acceleration

Fig.12 gives a schematic of the acceleration. A 20 m SFOFO matching section, using conventional RF, raises the beta functions to 1m prior to a 2.87 GeV solenoid focused superconducting RF linac. This linac is followed by a single, recirculating linear accel-

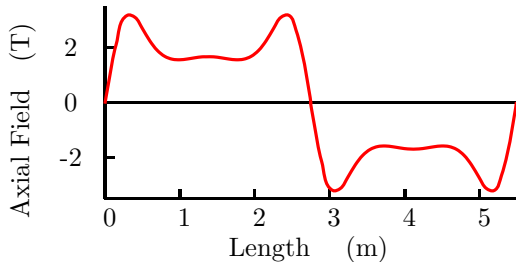


Figure 8: SFOFO lattice:the axial field vs. length.

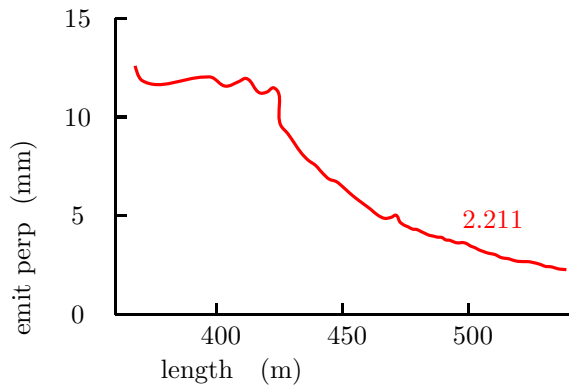


Figure 11: Transverse emittance vs length in cooling

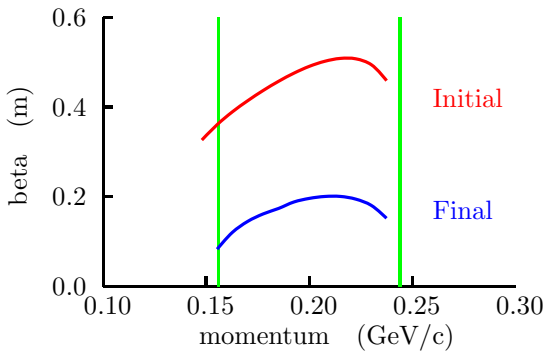


Figure 9: SFOFO lattice:  $\beta$  functions vs. momentum at the start and end of the channel.

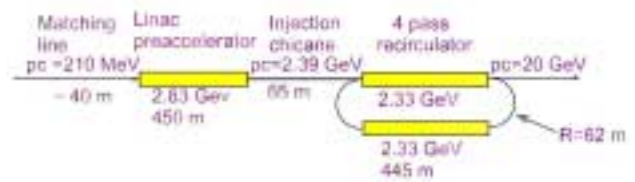


Figure 12: Acceleration schematic

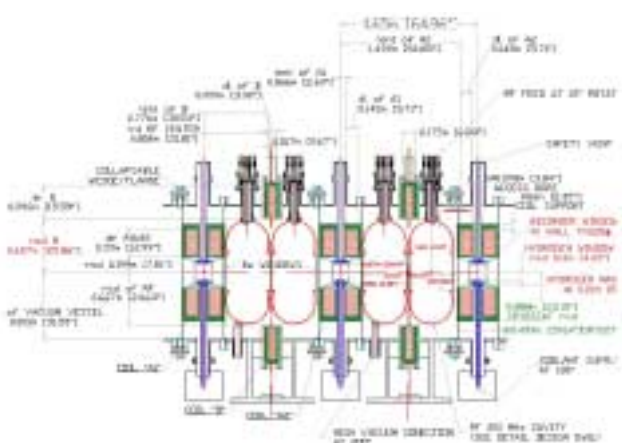


Figure 10: SFOFO Engineering section

erator (RLA) that raises the energy from 2.98 GeV to 20 GeV, in 4 passes. The RLA has separate arcs for each pass, but the beam passes through the same linac on each pass. The arcs have an average radius ranging from 81 m to 100 m. The final arc has an average bending field of 0.59 T.

## 2.7 Storage Ring

After acceleration, the muons are injected into the upward straight of a racetrack shaped storage ring. High field superconducting arc magnets are used at each end to minimize the arc length and maximize the fraction (35%) of muons that decay in the downward straight and generate neutrinos headed towards the detector at the WIPP facility in Carlsbad, 2903 km away. The muons, once injected, are never extracted, but are allowed to decay into electrons and neutrinos. The total heating from these electrons is 42 kW (126 W/m). This load is too high to be dissipated in the superconducting coils. A magnet design has been chosen[8] that allows the majority of these electrons to pass out between separate upper and lower cryostats, and be dissipated in a dump at room temperature. In order to keep the midplane free of superconducting coils in the arcs, the lattice uses skew quadrupoles for focusing. In order to maximize the average bending

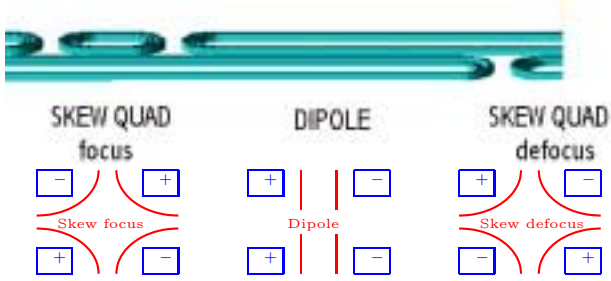


Figure 13: a) TOP: Storage ring coils; b) BOTTOM: conceptual cross-sections of focus, bending, and defocus magnets;

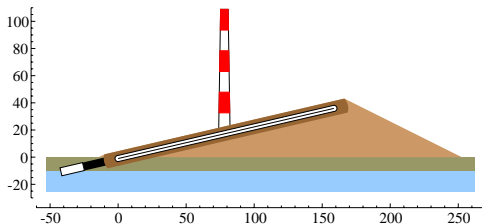


Figure 14: Cross section through ring and cover.

field, Nb<sub>3</sub>Sn pancake coils are employed, and in order to maximize the packing factor, one coil of the bending magnet is extended and used as one half of the previous or following skew quadrupole (fig.13).

Fig.14 shows a cross section of the ring which is kept above the water table and is covered by a 100 ft. high berm. The 300 ft. high BNL stack is also shown for scale.

### 3 PERFORMANCE

Complete simulations up to the start of acceleration have been performed by MARS[4] (for pion production) followed by ICOOL[9] (for transport, phase rotation and cooling). These have been confirmed by GEANT. They show 0.17 muons per initial proton on the target. i.e. 0.0071  $\mu$ 's / proton / proton energy in GeV. This can be compared with a value of 0.0011  $\mu$ 's / proton / proton energy in GeV in study 1[2]. The gain ( $\approx 6 \times$ ) comes from: a) The use of a mercury, instead of carbon, target ( $1.9 \times$ ); b) From the use of three, instead of a single, phase rotation induction linacs ( $2 \times$ ); c) from the tapered cooling design ( $1.4 \times$ ), and d) from a larger accelerator acceptance ( $1.2 \times$ ). The muons delivered to the ring with a 1 MW (4 MW) proton driver would be:

$$\mu/\text{year} =$$

$$10^{14}(\text{ppp}) \times 2.5(\text{Hz}) \times 10^7(\text{sec}) \times 0.17(\mu/p) \times 0.81(\text{acc}) \\ = 3.4 \ 10^{20} (= 14 \ 10^{20})$$

and the number of muons decaying in a straight sec-

tion would be:  
 $= 1.2 \ 10^{20}$  ( $= 4.8 \ 10^{20}$ ).

### 4 CONCLUSIONS

This Study 2 shows significant improvements ( $\approx 6 \times$ ) over Study 1, and there remain possibilities of further gains. Cooling of the longitudinal emittance [10] and the capture of both signs[11] appear possible and, together might improve overall performance by between 2 and 4. More study is needed. In addition, development and technical work is required on many of the components.

### 5 REFERENCES

- [1] J. Gallardo, <http://www.cap.bnl.gov/mumu/>
- [2] N. Holtkamp, D. Finley, Editors, "A Feasibility Study of a Neutrino Factory Based on a Muon Storage Ring", Aug., 2000 ([http://www.fnal.gov/projects/muon\\_collider/neutrino/fermi\\_study\\_after\\_april1st/](http://www.fnal.gov/projects/muon_collider/neutrino/fermi_study_after_april1st/))
- [3] C. Albright et al, "Physics at a Neutrino Factory", FERMILAB-FN-692, May, 2000.
- [4] N.V. Mokhov, "The MARS Code System User's Guide", Fermilab-FN-628 (1995) (<http://www-ap.fnal.gov/MARS/>); N.V. Mokhov, "Particle Yield and Radiation Fields in Feasibility Study-2 Target Capture System", MUC Note 0194, March 2001, (<http://www-mucool.fnal.gov/mcnotes/muc0194.ps>)
- [5] R. B. Palmer "Non-Distorting Phase Rotation", MUC Note 0114, April 2000, (<http://www-mucool.fnal.gov/notes/>)
- [6] Eun-San Kim et al, "LBNL Report on Simulation and Theoretical Studies of Muon Ionization Cooling", MUC Note 0036, July 1999; Eun-San Kim, M. Yoon, "Super FOFO cooling channel for a Neutrino Factory", MUC Note 0191, Feb. 2001 (<http://www-mucool.fnal.gov/notes/>)
- [7] M. J. Burns, et al, "DARHT Accelerators Update and Plans for Initial Operation" Proc. 1999 Acc. Conf., p. 617.
- [8] A. Skrinsky, "Towards Ultimate Polarized Muon Collider", AIP Conf. Proc. 441, 1997, p. 249
- [9] R. Fernow, <http://pubweb.bnl.gov/people/fernnow/icool/>
- [10] G. Hanson, ([http://needmore.physics.indiana.edu/~gail/emittance\\_exchange.html](http://needmore.physics.indiana.edu/~gail/emittance_exchange.html))
- [11] D. Neuffer "High Frequency Buncher and  $\phi - \delta E$  Rotation for the  $\mu^+ - \mu^-$  Source", MUCOOL Note 0181, Oct. 2000, (<http://www-mucool.fnal.gov/notes/>)